Early Warning of Abnormal Operating Modes Based on Feature Extraction from Cross-Section Frame at Discharge End for Sintering Process

Xinzhe Hao , Sheng Du * , Xian Ma , Mengxin Zhao

Posted Date: 16 June 2025

doi: 10.20944/preprints202506.1235.v1

Keywords: Abnormal operating mode; feature extraction; early-warning model; sintering process

 doi:10.20944/preprints202506.1235.v1

Article

Early Warning of Abnormal Operating Modes Based on Feature Extraction from Cross-section Frame at Discharge End for Sintering Process

Xinzhe Hao [1], Sheng Du [1,2,3,*], Xian Ma [1,2,3] and Mengxin Zhao [1]

[1] School of Automation, China University of Geosciences, Wuhan 430074, China
[2] Hubei Key Laboratory of Advanced Control and Intelligent Automation for Complex Systems, Wuhan 430074, China
[3] Engineering Research Center of Intelligent Technology for Geo-Exploration, Ministry of Education, Wuhan 430074, China
* Correspondence: dusheng@cug.edu.cn

Abstract: Abnormal operating modes in the iron ore sintering process often cause a decline in both the yield and quality of the resulting sinter ore. Accurate early warning of such modes is therefore essential for improving both the quantity and quality of sinter ore. This paper presents an early-warning method of abnormal operating mode based on the feature extraction from the cross-section frame at the discharge end. First, an edge-detection-based scheme is designed to isolate and analyze the red fire layer in the image. Second, a Random Forest feature importance ranking is employed to select process variables. Third, a Bayesian neural network is trained to build the early-warning model. Finally, the burn-through point is adopted as the classification criterion, and experiments are carried out on raw data collected from an industrial plant. The results show that the proposed method issues accurate early warnings of abnormal operating modes, achieving an accuracy of 94.07%, and thus offers promising prospects for industrial application.

Keywords: abnormal operating mode; feature extraction; early-warning model; sintering process

1. Introduction

Sintering is the principal route for producing high-quality synthetic iron ore. During sintering, base ore is blended with other materials to enrich desirable components and, through high-temperature reactions, to reduce impurities, thereby upgrading the product quality. The sinter ore produced through this process serves as the primary burden material for blast furnace ironmaking [1]. Global crude steel output reached 1.8826 billion tonnes in 2024 [2]. As steel demand continues to rise, high-grade natural ore alone can no longer satisfy industrial needs, making the sintering process increasingly critical.

Sintering is a thermal agglomeration operation whose principal feed materials are iron ore, returning sinter ore, fluxes and coke [3]. Its high energy consumption and severe environmental impact have long been major concerns for steel plants. An operating mode describes the state of process variables under specific conditions. Operators adjust control actions according to different modes to improve product quality, boost productivity and reduce energy use. Correctly identifying operating modes in the sintering process therefore has substantial economic value.

The recognition of abnormal operating modes has attracted considerable research attention, enabling mode-recognition methods to be applied to many industrial processes, the sintering process included [4]. Because manual monitoring is limited [5], production cannot always run safely. Hence, recognizing abnormal operating modes in industrial processes is crucial for operational safety. Tang et al. proposed an attention-based early warning framework for abnormal operating conditions in FCCU, combining denoising, Conv-LSTM, and anomaly attention modules to improve detection

 doi:10.20944/preprints202506.1235.v1

accuracy and robustness [6]. Du et al. clustered and smoothed sintering data with fuzzy C-means, built Naïve Bayes sub-models for mode recognition and combined them into a high-accuracy model, laying the groundwork for stable sinter quality [7]. However, their work did not consider the cross-section frame at the discharge end.

Recent studies have placed considerable emphasis on analyzing discharge end images in the context of iron ore sintering. In [8], a hybrid just-in-time soft sensing system was introduced to estimate carbon efficiency by extracting key features from cross-sectional frames. A genetic-algorithm-based fuzzy c-means clustering technique was applied to segment key frames into distinct regions, which then served as inputs for a soft sensor to predict the comprehensive carbon ratio (CCR) in real time. Liang et al. [9] proposed a CNN-Transformer dual-stream network for classifying sinter-flame combustion states with high accuracy. However, these approaches focused on combustion or efficiency analysis rather than early warning of abnormal operating modes.

Although the above methods achieved good experimental results, they still lack the use of the discharge end image for abnormal operating mode recognition, and they rarely provide early warning of modes. Issuing early warning of abnormal operating modes enables operators to intervene in advance, thereby shortening the time the strand spends in an abnormal state. Moreover, ignoring image features tends to reduce recognition accuracy.

To address the challenges in early detection of abnormal operating modes, this study proposes an early-warning model based on feature extraction from cross-sectional frames at the discharge end. The approach begins with frame segmentation to isolate the red fire layer, which is then analyzed separately. The Sobel edge detection algorithm is employed due to its balance of speed and accuracy, making it suitable for real-time industrial applications [10]. Subsequently, a one-way analysis of variance reveals that the continuity and height of the red fire layer are highly correlated with the operating mode. To further refine input selection, Random Forest feature importance analysis is performed, identifying the most relevant process variables. These top-ranked variables are used as inputs to a Bayesian Neural Network (BNN) model, which is trained to issue early warnings of abnormal operating modes. Real production data from an industrial sintering plant is utilized for model training and validation. Experimental results demonstrate that the proposed model achieves a prediction accuracy exceeding 94.07%, significantly outperforming existing methods referenced in [7] and [13].

The key contributions of this paper are summarized as follows:

(1) An early-warning method for abnormal operating modes that exploits feature extraction from the cross-section frame at the discharge end.
(2) A labelled, interpretable early-warning model that operators can readily accept for control guidance.
(3) An early-warning approach that combines Bayesian theory with operator experience, improving the reliability of the early-warning of abnormal operating mode.

2. Description of the Sintering Process and Design of the Early-Warning Scheme for Abnormal Operating Modes

This section first gives a detailed account of iron ore sinter production and of the characteristics of the cross-section frame at the discharge end. On the basis of production requirements, an early-warning scheme for abnormal operating modes is then formulated.

2.1. Description of the Iron Ore Sintering Process

The iron ore sintering process is multivariate, highly nonlinear and strongly time-delayed, and it can switch among several operating modes [11]. The Dwight-Lloyd sintering machine remains the dominant equipment used in current sintering operations. In this study, a 360 m^2 strand with 24 bellows is selected as the case example. The overall iron ore sintering process is illustrated in Figure 1.

 doi:10.20944/preprints202506.1235.v1

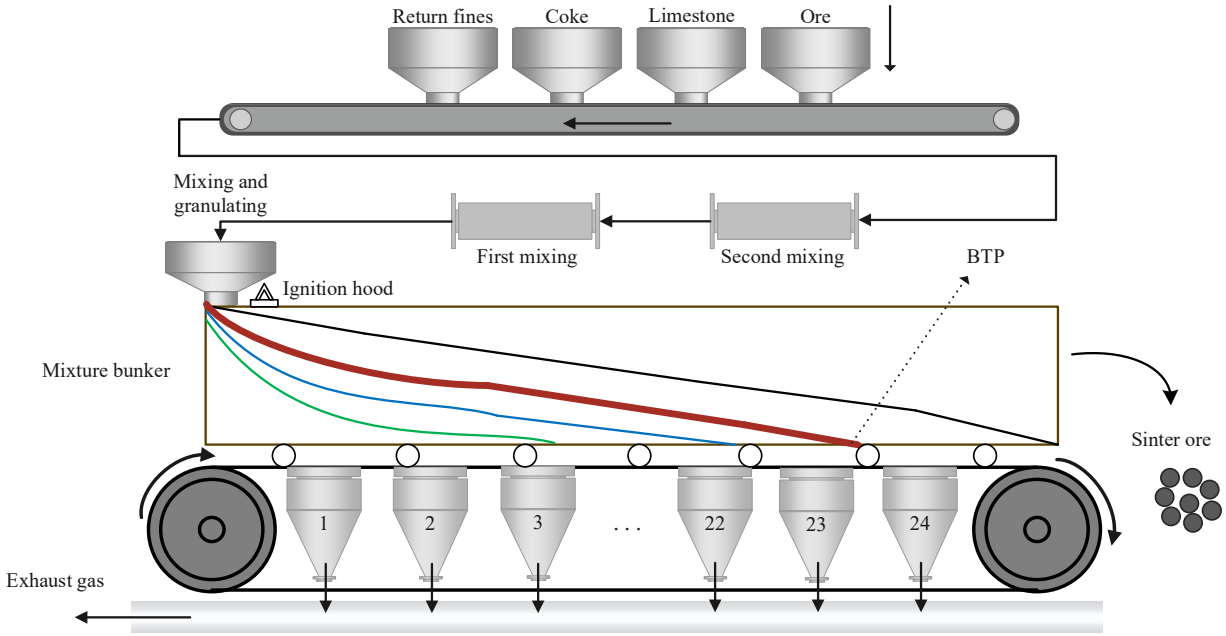

Figure 1. Iron ore sintering process.

The process agglomerates iron ore, returning sinter ore, fluxes and coke into hot sinter ore [12]. Raw materials are first blended with water in fixed proportions to form a mixture that is stored in a mixing hopper. A roll feeder then distributes the mixture onto a moving pallet strand. Inside the ignition hood the charge is ignited, after which down-draft fans draw combustion air so that the bed burns progressively from top to bottom. When the leading edge of the combustion zone reaches the grate bars, the mixture has burned out and the process reaches the burn-through point (BTP); combustion then ceases. Under the normal operating mode, the BTP coincides with approximately the 23rd bellows.

Operators judge process stability mainly by tracking the BTP. Because the BTP marks the location where the mixture has finished burning, its position is the most important thermal indicator. If the BTP appears upstream of the target position, the effective bed area is not fully utilized and strand productivity falls. If the BTP appears downstream, the bed has not burned through at discharge, which increases the recycle load of returning sinter ore. Hence, the current operating mode can be assessed directly from the BTP position [13].

After complete combustion, the hot bed travels roughly one additional bellows length and reaches the segmentation frame. Here the sinter cake is broken loose and discharged. When the cake has fallen away completely, the cross-section frame at the discharge end becomes fully visible, providing the image used in this study. A typical bellows exhaust gas temperature profile is shown in Figure 2.

 doi:10.20944/preprints202506.1235.v1

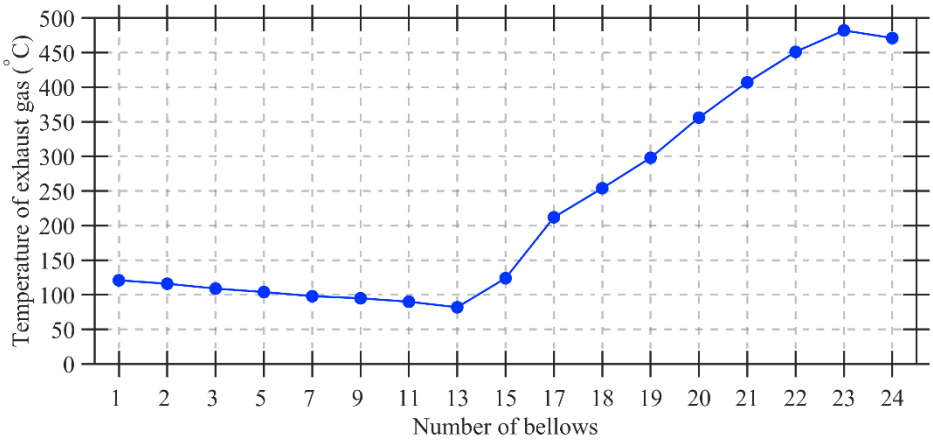

Figure 2. Temperature of the exhaust gas in bellows.

2.2. Characteristic Analysis of Sintering Process

Before applying the cross-section frame at the discharge end for early warning of abnormal operating modes, it is essential to examine its correlation with the operating mode and to clarify the challenges involved in accurate early warning.

At the discharge end, the captured cross-section frame reveals three distinct zones: the red fire layer, the background area and the trolley baffle. Thermally, the strand can run in one of three operating modes—over-burning, normal or under-burning [14]. Over-burning arises when the cake reaches burn-through ahead of schedule, pushing the BTP upstream. Under-burning occurs when combustion remains incomplete, so the BTP shifts downstream. Either deviation diminishes strand utilization and lowers sinter quality, thereby impairing subsequent blast-furnace performance [15].

The red fire layer provides the clearest visual cue to the combustion state. Two attributes—its vertical height and its continuity—define that state. A tall, unbroken red band indicates an elevated combustion front, under-burning of the mix and a delayed BTP; a shallow, intermittent band signals premature burn-through and an advanced BTP. When both height and continuity are intermediate, the bed burns out at the intended depth. Thus, every operating mode is associated with a characteristic red fire layer pattern.

The location of BTP (L_{BTP}) is taken as the indicator of the operating mode. In normal operation L_{BTP} must lie inside the band $[L_d - d, L_d + d]$, where L_d is the target BTP position and d the admissible fluctuation (here $d = 0.5$ and $L_d = 22.5$). If L_{BTP} rises above the upper limit the bed is under-burned; if it falls below the lower limit the bed is over-burned.

Thus, three modes are defined:

OM_1—Over-burning: $L_{\mathrm{BTP}} < L_d - d$.

Premature burn-through lowers strand utilization and reduces sinter output.

OM_2—Normal: $L_d - d \le L_{\mathrm{BTP}} \le L_d + d$.

The mixture burns out precisely at the desired location, fulfilling production requirements.

OM_3—Under-burning: $L_{\mathrm{BTP}} > L_d - d$.

Incomplete burn-through of the mixture at the time of unloading results in reduced output and inferior sinter ore quality.

When over-burning occurs, combustion ends early; the red fire layer reaches the grate, giving a low and intermittent appearance. When under-burning occurs, the combustion zone remains in the upper–middle bed; the red fire layer appears high and continuous. Under normal operating mode the red fire layer is located in the middle-lower part of the frame and shows good continuity.

2.3. Design of the Early-Warning Scheme for Abnormal Operating Modes

 doi:10.20944/preprints202506.1235.v1

Given the strong non-linearity and high degree of coupling inherent in the sintering process [16], this study proposes an early-warning model for abnormal operating modes that leverages the cross-section frame at the discharge end. To ensure reliable early warning, it is crucial to fully incorporate the relevant state parameters into the model. Because the key frame features are also highly correlated with the operating mode, they must be included among the model inputs.

The early-warning scheme comprises three main steps. First, an image-processing module is designed to extract feature parameters from the discharge end cross-section frame. Next, a Random Forest feature importance ranking is applied to select the variables. Then, a BNN is constructed to serve as the early-warning model. The overall structure is shown in Figure 3.

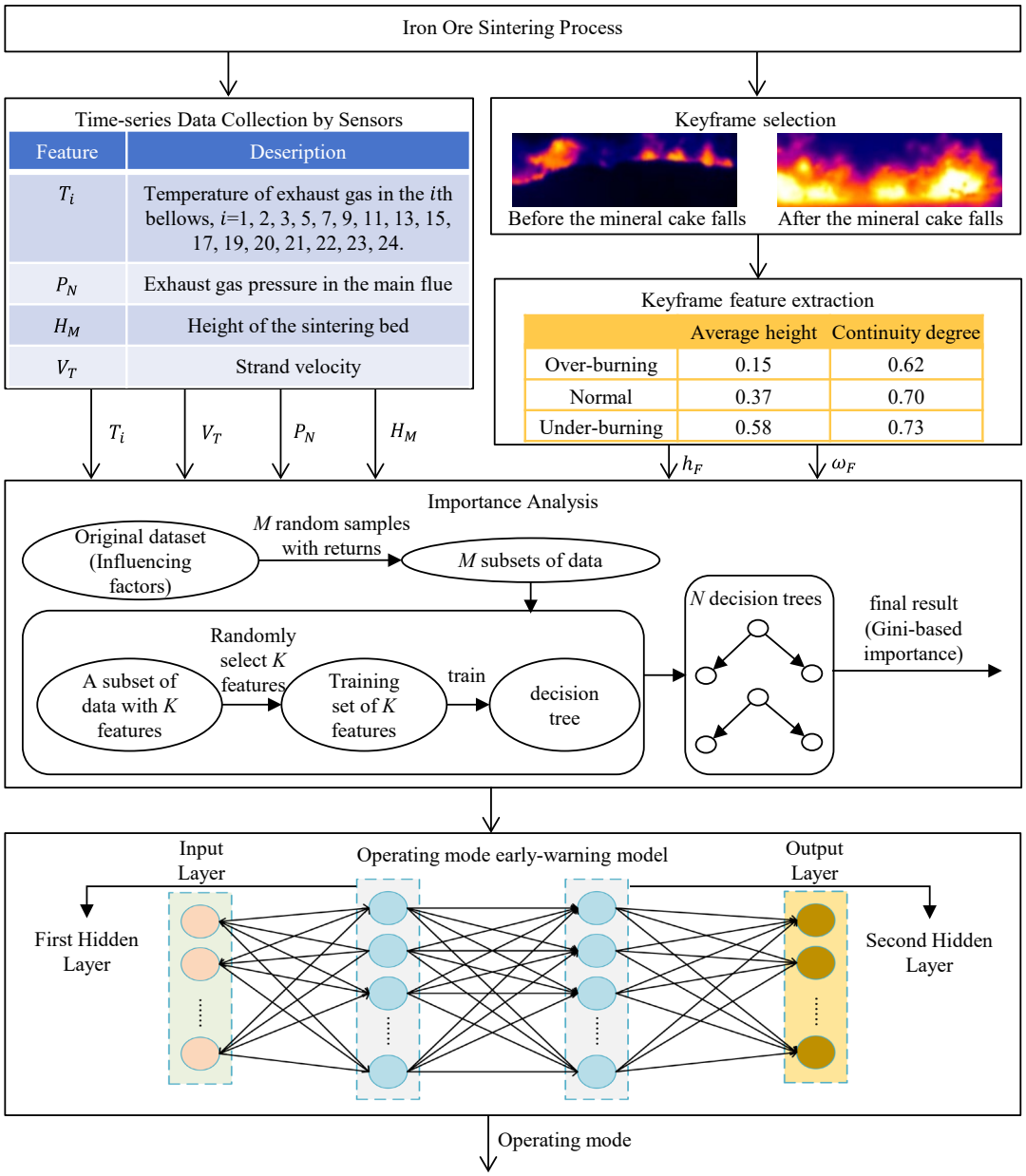

Figure 3. Operating mode early-warning model for sintering process.

For the model inputs, the key frame features are extracted first. In view of the periodic descent of the sinter cake, a key frame selection strategy is devised. After selecting the discharge end key frame, the Sobel operator segments it into the red fire layer and the background region. The resulting feature parameters are calculated and stored in a database.

To handle the multi-factor influences on the operating mode, a Random Forest algorithm is employed to compute the importance of each variable. Random Forest is simple, easy to implement

 doi:10.20944/preprints202506.1235.v1

and incurs only modest computational cost; variables with higher importance scores are retained as inputs to the early-warning model.

Finally, a BNN-based early-warning model is used, taking as inputs the feature parameters of the discharge end frame together with several key state parameters of the sintering process. The BNN is chosen because it merges the strengths of Bayesian statistics and neural networks, thereby enhancing both early-warning accuracy and generalization ability.

3. Early-Warning Model for Abnormal Operating Modes

This section establishes the early-warning model for abnormal operating modes. First, an image-processing module is used to extract feature parameters from the cross-section frame at the discharge end. Second, a Random Forest feature importance ranking is applied to select the input variables. Finally, a BNN is trained to construct the early-warning model.

3.1. Feature extraction from the cross-section frame at the discharge end

A key frame selection method was designed according to the characteristics of the infrared video taken at the discharge end. The key frame extraction procedure processes the images captured at the discharge end in order to identify those moments that best represent changes in the operating mode. A camera mounted at the discharge end continuously records the sintering process, and, during processing, only the key frames that have a significant influence on the operating mode are retained.

The sinter cake falls from the pallet at roughly 60 s intervals; immediately afterwards a large dust plume is generated, degrading image quality. To avoid this problem, the key frame is extracted during the initial appearance of the red fire layer, before dust obscures the view. In the present study an image is captured every 5 s, and the grey-level difference between successive frames is calculated. The frame with the maximum difference is selected as the key frame because it clearly reflects the operating mode while minimizing dust interference, ensuring both efficiency and accuracy.

Information from the red fire layer is essential for early warning, so this region must be segmented before the image features are calculated. Sobel edge detection, a classical image-processing algorithm, identifies edges by evaluating the gradient magnitude and direction at each pixel, and is applied in this study to segment the key frames. A comparison of the frame before and after the sinter cake has fallen is shown in Figure 4.

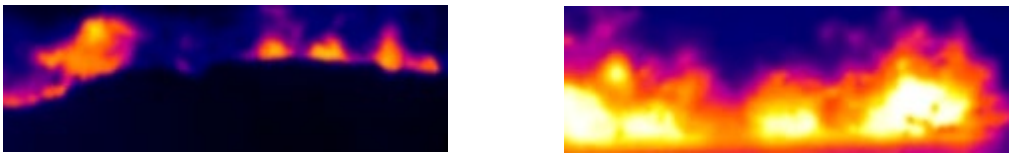

(**a**) Before the mineral cake falls (**b**) After the mineral cake falls

Figure 4. Comparison of sintered ore cake before and after falling.

As outlined in Section 2.2, two descriptors are extracted from each key frame: the average height h and the continuity degree ω of the red fire layer.

The average height is obtained by

$$h = \frac{1}{k}\sum_{i=1}^{k} y_i, \tag{1}$$

where y_i denotes the highest pixel ordinate in the $i-th$ column and k is the total number of columns.

Continuity is measured via

$$\omega = \frac{n_p}{k}, \tag{2}$$

with n_p representing the count of columns whose red fire layer height reaches (or exceeds) that average value, while k again is the column total.

 doi:10.20944/preprints202506.1235.v1

Thus, h captures the vertical extent of the red zone, whereas ω quantifies how consistently that height is maintained across the frame.

3.2. Input Variable Selection of Early-Warning Model

The sintering data set contains 20 measured variables, as shown in Figure 3. To address the multifactor influence on the operating mode, a Random Forest algorithm is employed to evaluate the importance of each variable. Random Forest is an ensemble method that builds multiple decision trees as base learners and aggregates their outputs to improve performance. It improves the classification performance of single trees by bootstrap aggregation and random feature splitting during tree construction [18]. It is straightforward to implement and has low computational cost.

To quantify the contribution of each variable to the classification process, the Gini index is used as the splitting criterion in the Random Forest algorithm. For any node m in a decision tree within the Random Forest, the Gini impurity g_m is defined as:

$$g_m = \sum_{k=1}^{K} \hat{p}_{mk}(1 - \hat{p}_{mk}), \tag{3}$$

where K is the total number of classes, $\hat{p}_{mk}$ is the estimated probability that a sample at node m belongs to class k.

For binary classification problems, this can be simplified as:

$$g_m = 2\hat{p}_m(1 - \hat{p}_m). \tag{4}$$

If a variable t_j is used in the $i-th$ decision tree and contributes to M splits, then the importance score v_{ij} of variable t_j in that tree, based on the reduction in Gini impurity, is given by:

$$v_{ij}^{(\text{Gini})} = \sum_{m=1}^{M} \Delta g_{jm}^{(\text{Gini})}, \tag{5}$$

where $\Delta g_{jm}^{(\text{Gini})}$ is the reduction in Gini impurity at node m when splitting on variable t_j.

The total importance of variable t_j across all n trees in the Random Forest is calculated as the average:

$$v_j^{(\text{Gini})} = \frac{1}{n}\sum_{i=1}^{n} v_{ij}^{(\text{Gini})}. \tag{6}$$

This quantitative metric enables Random Forest to rank variables by their contribution to the classification outcome, making it suitable for selecting relevant features that influence the sintering process''s operating mode. Variables with relatively high Gini importance values were chosen as input features for the early-warning model. The corresponding importance coefficients are shown in Table 1.

Table 1. Results of importance analysis.

Feature	T_{23}	V_T	T_{21}	P_N	H_M	T_{22}	T_{24}
Gini-based importance	0.402	0.356	0.341	0.305	0.302	0.282	0.279
Feature	T_{17}	T_{20}	T_{11}	T_1	T_{18}	T_3	T_9
Gini-based importance	0.233	0.198	0.153	0.149	0.098	0.071	0.032

To accelerate the early-warning model, the number of selected inputs must be limited. In order to avoid excessive redundancy while still retaining sufficient time series information, an importance score threshold of 0.3 is adopted; the resulting scores are listed in Table 2. The analysis shows that

 doi:10.20944/preprints202506.1235.v1

temperature of exhaust gas in 23rd bellows ($\boldsymbol{T_{23}}$), $\boldsymbol{T_{21}}$, the strand speed, the main flue negative pressure and the bed height all have importance values above the threshold. These five variables are therefore chosen as the inputs to the abnormal operating mode early-warning model.

Table 2. Cross-section frames at discharge end features analysis.

Operating mode	Average height	Continuity degree
Over-burning	0.15	0.62
Normal	0.37	0.70
Under-burning	0.58	0.73

3.3. Structure of Early-Warning Model

The early-warning model for sintering operating mode is designed to infer the upcoming state OM_k $(k \in \{1,2,3\})$ using a set of real-time process parameters. The selected parameter vector $P_{\text{in}} \in R^d$, obtained from prior feature selection, serves as the model input, and the early-warning result represents the output.

BNNs integrate the interpretability of Bayesian statistics with the expressive power of deep learning [19]. Traditional Bayesian models rely on Bayes' theorem to update probability estimates by combining prior distributions with observed data. However, they struggle with scalability in high-dimensional, nonlinear contexts. Neural networks, on the other hand, are effective at abstracting complex patterns but lack inherent uncertainty quantification. BNNs overcome both limitations by treating all weights and biases as probability distributions rather than fixed values, allowing them to represent model uncertainty and reduce overfitting.

Formally, the transformation in each layer l of a BNN is defined as:

$$a^{(l)} = \sigma\left(W^{(l)}a^{(l-1)} + b^{(l)}\right), \tag{7}$$

where $W^{(l)}$ and $b^{(l)}$ are random variables drawn from prior distributions, $\sigma(\cdot)$ denotes the activation function, and $a^{(0)} = P_{\text{in}}$ is the input feature vector.

To approximate the intractable posterior $p(W, b|\mathcal{D})$, variational inference is used:

$$p(W, b \mid \mathcal{D}) \approx q(W, b \mid \theta), \tag{8}$$

where $q(\cdot)$ is a tractable variational distribution parameterized by θ, and $\mathcal{D}$ is the dataset.

The objective is to minimize the evidence lower bound (ELBO):

$$\mathcal{L} = E_q[\log p(\mathcal{D} \mid W, b)] - \mathrm{KL}\left(q(W, b) \parallel p(W, b)\right), \tag{9}$$

This balances data fit and model complexity, enabling better generalization and robustness. The architecture of the complete early-warning system is illustrated in Figure 5.

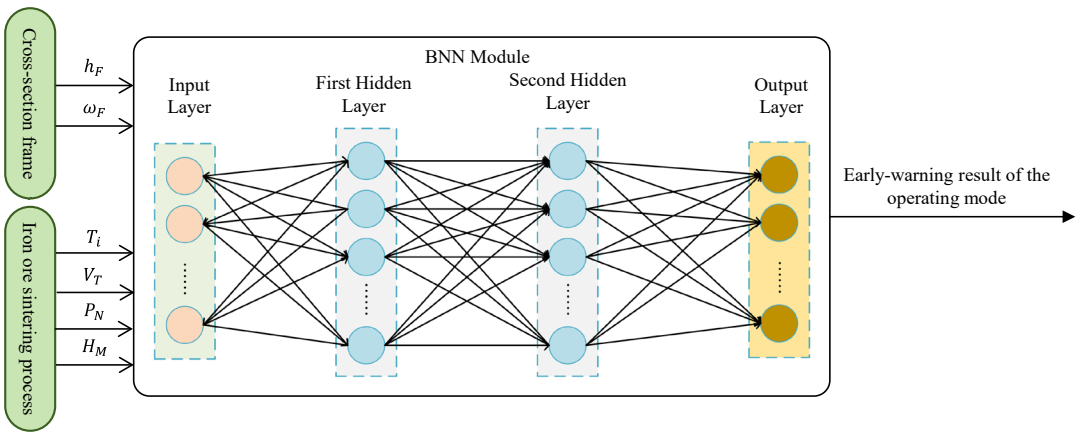

Figure 5. Structure of abnormal operating modes early-warning model.

 doi:10.20944/preprints202506.1235.v1

4. Experimental Study and Analysis

This section validates the proposed early-warning method for abnormal operating modes by means of experiments based on raw data collected from a steel plant and discusses the results.

4.1. Experimental Design

To validate the effectiveness of the proposed early-warning scheme utilizing cross-section frame features at the discharge end, a series of images at the discharge end were collected from an actively operating industrial strand. Key frames were identified in the infrared video—captured with IRTool Pro—by applying the selection strategy described above. After saving the raw stream to a local directory, a Python routine (i) isolated the key frames, (ii) defined crop coordinates and (iii) automatically clipped the region of interest, namely the red fire layer. Each cropped frame was then passed through image-segmentation and feature-extraction steps, and the resulting parameters were written back to disk by the same Python script.

Because the field sensors sample every 5 s, the sampling interval of the raw production data was enlarged to 1 min to reduce the influence of high-frequency noise. In total, 3000 time series samples were collected: the training set consists of 1000 over-burning, 1000 normal and 1000 under-burning cases, while the remaining 540 samples—180 for each operating mode—were set aside for testing.

Each key frame was segmented with the Sobel edge-detection method. Frames corresponding to the three operating modes—identified in consultation with experienced plant operators—were selected for segmentation. The results are presented in Figure 6, where it is evident that the red fire layer exhibits distinct characteristics across the three operating modes: under over-burning the layer's continuity and average height are markedly lower than in the normal mode, whereas under-burning yields the greatest height and continuity. The numerical feature parameters for the three frames depicted in Figure 6 are provided in Table 2.

To refine the experimental results, multiple runs were performed. Once the features of the cross-section frame at the discharge end had been extracted, they were merged with the time series process data to serve as the input vector of the abnormal operating mode early-warning model, which then produced the early-warning result for the operating mode.

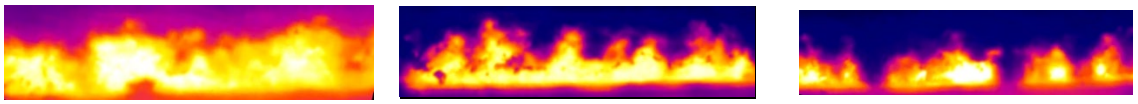

(**a**) Original figure(under-burning) (**b**) Original figure(normal) (**c**) Original figure(over-burning)

Figure 6. Image segmentation result.

The early-warning performance for different operating modes is represented by the confusion matrix in Table 3. In this matrix, $M_{ij}(i = 1,2,3; j = 1,2,3)$ denotes the number of test samples that are predicted as operating mode OM_i by the early-warning model, while their true label is OM_j. In addition, three metrics are defined to evaluate the early-warning performance: η_a represents the overall accuracy, η_f the false-alarm rate, and η_m the missing-alarm rate. They are expressed as,

$$\eta_a = \frac{M_{11} + M_{22} + M_{33}}{\sum_{i=1}^{3}\sum_{i=1}^{3} M_{ij}} \times 100\%. \tag{10}$$

$$\eta_f = \frac{M_{12} + M_{32}}{\sum_{i=1}^{3} M_{i2}} \times 100\%. \tag{11}$$

$$\eta_f = \frac{M_{21} + M_{31} + M_{13} + M_{23}}{\sum_{i=1}^{3} M_{i1} + \sum_{i=1}^{3} M_{i3}} \times 100\%. \tag{12}$$

Table 3. Example of confusion matrix.

 doi:10.20944/preprints202506.1235.v1

	Mode	Actual			Accuracy	False-alarm rate	Missing-alarm rate
		OM_1	OM_2	OM_3			
Early-warning	OM_1	M_{11}	M_{12}	M_{13}	η_a	η_f	η_m
	OM_2	M_{21}	M_{22}	M_{23}			
	OM_3	M_{31}	M_{32}	M_{33}			

4.2. Experimental Result Analysis

The operating mode defined by L_{BTP} is used as the recognition target. To evaluate the early-warning accuracy more effectively, the metrics introduced above are applied to verify the validity of the proposed early-warning model for abnormal operating modes.

In addition, two comparative experiments are established to highlight the advantages of the proposed method based on feature extraction from the cross-section frame at the discharge end. The model presented in [7] is designed for operating mode recognition in the iron ore sintering process and is constructed using a Naïve Bayes classifier, making it comparable to our method in terms of its probabilistic framework. The model in [13] employs a fuzzy rule-based framework to predict operating modes for the same process, sharing essentially the same background and objective as the present study. Therefore, these two models are adopted as benchmarks for comparison with our proposed approach. According to Table 4, our model exhibits the best performance in terms of mean accuracy. A reliable early-warning model for operating mode should ideally combine high accuracy with both a low false-alarm rate and a low missing-alarm rate. Our model surpasses the models in [13] and [7] in all three metrics—accuracy, false-alarm rate, and missing-alarm rate. Hence the proposed approach is effective. It offers operators a reliable reference for adjusting strand operation and thus holds significant practical value for enhancing combustion efficiency and boosting productivity in the sintering process.

Table 4. Early-warning result of operating mode.

Model	Mode	OM_1	OM_2	OM_3	η_a	η_f	η_m
Model in [7]	OM_1	123	42	15	79.63%	25.71%	17.81%
	OM_2	1	130	49			
	OM_3	0	3	177			
Model in [13]	OM_1	153	14	13	86.85%	9.33%	14.62%
	OM_2	2	136	42			
	OM_3	0	0	180			
Our model	OM_1	162	10	8	94.07%	6.67%	5.56%
	OM_2	1	168	11			
	OM_3	0	2	178			

The comparison of false-alarm rate and missing-alarm rate results are shown in Figure 7. Our model achieves both a lower false-alarm rate η_f and missing-alarm rate η_m compared to the benchmarks. The false-alarm rate increases computational burden and may trigger unnecessary control actions, while the missing-alarm rate risks failing to address actual abnormal conditions. Since intelligent decision-making depends on early-warning outputs, reducing η_m is especially critical for maintaining process stability. The comparison between false-alarm and missing-alarm rates across different algorithms is shown in Figure 7. It is evident that the proposed model outperforms the benchmark methods in both false-alarm and missing-alarm rates.

 doi:10.20944/preprints202506.1235.v1

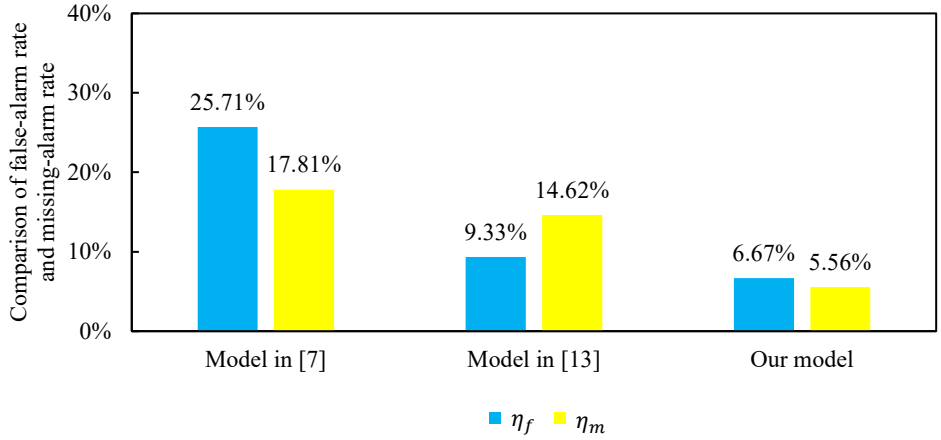

Figure 7. Comparison of false-alarm rate and missing-alarm rate among different algorithms.

5. Conclusions

Reliable early warning of abnormal operating modes is vital for correctly characterizing the combustion state of a sintering strand and for keeping the process under stable control. In this study we begin by devising a dedicated feature-extraction routine for the discharge end cross-section frame, and then built an abnormal operating mode early-warning model based on a BNN. Compared with other models, the proposed early-warning model provides higher accuracy. Overall, the early-warning model that relies on image features from the discharge end constitutes an effective guide for sinter production and offers tangible benefits for plants aiming to cut costs while boosting operational efficiency. Looking ahead, the framework could be coupled with an intelligent control layer to adjust the operating mode automatically.

Despite its high-precision warning performance, the approach still has two notable shortcomings:

(1) It relies on an on-site, high-temperature infrared camera to obtain the key frames required for real-time warnings.

(2) Because of the harsh working environment, discharge end images are sometimes blurred, which can degrade the accuracy of the warning results.

Author Contributions: Conceptualization, S.D.; Methodology, X.H. and S.D.; software, X.H.; Validation, X.H.; Investigation, X.M. and M.Z.; data curation, X.M. and M.Z.; Writing—original draft, X.H.; Writing—review & editing, X.H., X.M., and S.D.; Project administration, S.D.; Funding acquisition, X.H. and S.D. All authors have read and agreed to the published version of the manuscript.

Funding: This work was supported in part by the Hubei Provincial Natural Science Foundation of China under Grant No. 2025AFB471, the Natural Science Foundation of Wuhan under Grant No. 2024040801020280, and in part by the Fundamental Research Funds for the Central Universities, China University of Geosciences under Grant No. 2021237.

Institutional Review Board Statement: Not applicable.

Informed Consent Statement: Not applicable.

Data Availability Statement: The authors do not have permission to share data.

Conflicts of Interest: The authors declare that they have no known competing financial interests or personal relationships that could have appeared to influence the work reported in this paper.

References

 doi:10.20944/preprints202506.1235.v1

1. Hu, J.; Li, H.; Li, H.; Wu, M.; Cao, W.; Pedrycz, W. Relevance vector machine with hybrid-kernel soft sensor via data augmentation for incomplete output data in the sintering process. Control Engineering Practice 2024, 145, 105850. https://doi.org/10.1016/j.conengprac.2024.105850
2. World Steel Association. December 2024 crude-steel production and 2024 global totals. Available online: https://worldsteel.org/zh-hans/media/press-releases/2025/december-2024-crude-steel-production-and-2024-global-totals/ (accessed on 24 January 2024).
3. Fernández-González, D.; Ruiz-Bustinza, I.; Mochón, J.; González-Gasca, C.; Verdeja, L.F. Iron-ore sintering: Process. Mineral Processing and Extractive Metallurgy Review 2017, 38, 215–227. https://doi.org/10.1080/08827508.2017.1288115
4. Bazart, L.; Maquin, D.; Khelassi, A.; Bèle, B.; Ragot, J. Operating-mode recognition: Application in continuous casting. In Proceedings of the IEEE Conference on Control and Fault-Tolerant Systems (SysTol 2013); IEEE: Nice, France, 9–11 October 2013; pp. 790–795. https://doi.org/10.1109/SysTol.2013.6693911
5. Hwang, D.H.; Han, C. Real-time monitoring for a process with multiple operating modes. Control Engineering Practice 1999, 7, 891–902. https://doi.org/10.1016/S0967-0661(99)00038-6
6. Tang, C.; Huang, J.; Xu, M.; Liu, X.; Yang, F.; Feng, W.; He, Z.; Lv, J. Attention-based early warning framework for abnormal operating conditions in fluid catalytic cracking units. Applied Soft Computing 2024, 153, 111275. https://doi.org/10.1016/j.asoc.2024.111275
7. Du, S.; Wu, M.; Chen, L.; Cao, W.; Pedrycz, W. Operating-mode recognition based on clustering of time-series data for the iron-ore sintering process. Control Engineering Practice 2020, 96, 104297. https://doi.org/10.1016/j.conengprac.2020.104297
8. Chen, X.; She, J. A hybrid just-in-time soft sensor for carbon efficiency of the iron-ore sintering process based on feature extraction of cross-sectional frames at the discharge end. Journal of Process Control 2017, 54, 14–24. https://doi.org/10.1016/j.jprocont.2017.01.006
9. Liang, X.; An, J.; Cao, X.; et al. Classification of combustion state of sintering flame based on a CNN-Transformer dual-stream network. Journal of Applied Optics 2023, 44, 1030–1036. https://doi.org/10.5768/JAO202344.0502003
10. Zhang, J.Y.; Chen, Y.; Huang, X.X. Edge detection of images based on an improved Sobel operator and genetic algorithms. In Proceedings of the 2009 International Conference on Image Analysis and Signal Processing (IASP 2009); IEEE: Linhai, China, 11–12 April 2009; pp. 31–35. https://doi.org/10.1109/IASP.2009.5054605
11. Wu, M.; Xu, C.; She, J.; Cao, W. Neural-network-based integrated model for predicting the burn-through point in a lead–zinc sintering process. Journal of Process Control 2012, 22, 925–934. https://doi.org/10.1016/j.jprocont.2012.03.007
12. Chen, X.; Hu, Y.; Liu, C.; Chen, A.; Chi, Z. Dynamic spatio-temporal graph network based on multi-level feature interaction for sinter TFe prediction. Journal of Process Control 2025, 148, 103401. https://doi.org/10.1016/j.jprocont.2025.103401
13. Du, S.; Wu, M.; Chen, L.; et al. An intelligent decision-making strategy based on the forecast of abnormal operating mode for the iron-ore sintering process. Journal of Process Control 2020, 96, 57–66. https://doi.org/10.1016/j.jprocont.2020.11.001
14. Hu, J.; Wu, M.; Chen, L.; Cao, W.; Pedrycz, W. Real-time dynamic prediction model of carbon efficiency with working-condition identification in the sintering process. Journal of Process Control 2022, 111, 97–105. https://doi.org/10.1016/j.jprocont.2022.02.002
15. Li, H.; Wu, M.; Du, S.; et al. Prediction model of burn-through point with data correction based on feature matching of cross-section frame at the discharge end. Journal of Process Control 2024, 140, 103265. https://doi.org/10.1016/j.jprocont.2024.103265
16. Chen, X.; Liu, C.; Xia, H.; Chi, Z. Burn-through point prediction and control based on multi-cycle dynamic spatio-temporal feature extraction. Control Engineering Practice 2025, 154, 106165. https://doi.org/10.1016/j.conengprac.2024.106165
17. Du, S.; Ma, X.; Fan, H.; et al. Intelligent prediction and soft sensing of comprehensive production indicators for iron-ore sintering: A review. Computers in Industry 2025, 165, 104215. https://doi.org/10.1016/j.compind.2024.104215

 doi:10.20944/preprints202506.1235.v1

18. Chen, R.C.; Dewi, C.; Huang, S.W.; Caraka, R.E. Selecting critical features for data classification based on machine-learning methods. Journal of Big Data 2020, 7, 52. https://doi.org/10.1186/s40537-020-00327-4
19. Wang, K.; Du, H.; Jia, R.; Jia, H. Performance comparison of a Bayesian deep-learning model and a traditional Bayesian neural network in short-term PV interval prediction. Sustainability 2022, 14, 12683. https://doi.org/10.3390/su141912683